

Predicting Multi-Component Phase Equilibria of Polymers using Approximations to Flory–Huggins Theory

Citation for published version (APA):

van Leuken, S. H. M., van Benthem, R. A. T. M., Tuinier, R., & Vis, M. (2023). Predicting Multi-Component Phase Equilibria of Polymers using Approximations to Flory–Huggins Theory. *Macromolecular Theory and Simulations*, 32(4), Article 2300001. <https://doi.org/10.1002/mats.202300001>

DOI:

[10.1002/mats.202300001](https://doi.org/10.1002/mats.202300001)

Document status and date:

Published: 01/07/2023

Document Version:

Publisher's PDF, also known as Version of Record (includes final page, issue and volume numbers)

Please check the document version of this publication:

- A submitted manuscript is the version of the article upon submission and before peer-review. There can be important differences between the submitted version and the official published version of record. People interested in the research are advised to contact the author for the final version of the publication, or visit the DOI to the publisher's website.
- The final author version and the galley proof are versions of the publication after peer review.
- The final published version features the final layout of the paper including the volume, issue and page numbers.

[Link to publication](#)

General rights

Copyright and moral rights for the publications made accessible in the public portal are retained by the authors and/or other copyright owners and it is a condition of accessing publications that users recognise and abide by the legal requirements associated with these rights.

- Users may download and print one copy of any publication from the public portal for the purpose of private study or research.
- You may not further distribute the material or use it for any profit-making activity or commercial gain
- You may freely distribute the URL identifying the publication in the public portal.

If the publication is distributed under the terms of Article 25fa of the Dutch Copyright Act, indicated by the "Taverne" license above, please follow below link for the End User Agreement:

www.tue.nl/taverne

Take down policy

If you believe that this document breaches copyright please contact us at:

openaccess@tue.nl

providing details and we will investigate your claim.

Predicting Multi-Component Phase Equilibria of Polymers using Approximations to Flory–Huggins Theory

Stijn H. M. van Leuken, Rolf A. T. M. van Benthem, Remco Tuinier,* and Mark Vis*

The rational development of sustainable polymeric materials demands tunable properties using mixtures of polymers with chemical variations. At the same time, the sheer number of potential variations and combinations makes experimentally or numerically studying every new mixture impractical. A direct predictive tool quantifying how material properties change when molecular features change provides a less time- and resource-consuming route to optimization. Numerically solving Flory–Huggins theory provides such a tool for mono-disperse mixtures with a limited number of components, but for multi-component systems the large number of equations makes numerical computations challenging. Approximate solutions to Flory–Huggins theory relating miscibility and solubility to molecular features are presented. The set of approximate relations show a wider range of accuracy compared to existing approximations. The combination of the analytical, lower-order, and more accurate higher-order approximations together contribute to a broader applicability and extensibility of Flory–Huggins theory.

optimize material properties. However, the phase stability of such mixtures must be taken into account. The equilibrium concentrations in the different phases of these systems provide insight into the solubility,^[5] solvent uptake in polymer melts,^[6] maximum concentrations in immiscible polymer blends,^[7] and equilibrium concentrations upon phase-separation^[8]—all properties that are important for the processing and application of materials, aiding the explanation of experimental observations.

A wide range of experimental methods has been developed and used to study the phase-separation of polymers. Calorimetry,^[9] scattering,^[10] spectroscopy,^[11] vapor and gas sorption,^[12] inverse gas chromatography,^[13] melting point depression,^[14] non-radiative energy transfer,^[15] and excimer fluorescence^[16]

can all be used to measure quantities relevant for the miscibility of polymers.^[17,18] However, the large number of possible polymer mixtures makes it impossible to test all combinations experimentally. Additionally, challenges such as precise sample preparation, detection of phase transitions, and measuring other material properties make it challenging to obtain all the relevant information, even for experimentally tested combinations of polymers.^[19] Theoretical frameworks relating unknown material properties to known material properties and predicting their dependency on molecular features helps to understand these systems better. Such frameworks guide the design of bio-based and circular materials and the choice for the most insightful experiments, reducing the required number of experiments.


Theory and simulation have been used often to predict and explain the phase behavior of polymers. Commonly used simulation methods are based on molecular dynamics simulations^[20] and Monte Carlo simulations.^[21] A problem with using simulations to determine equilibrium concentrations of polymers is that the time to reach equilibrium scales with the size of the polymers. Therefore, simulations become extremely computationally demanding for realistic systems. In molecular dynamics simulations, the overall movement of polymers slows down with polymer length, particularly above the entanglement length.^[22] Molecular dynamics simulations with larger polymers become possible by simplifying interaction potentials, course-graining, and multi-scale sampling.^[23,24] The achievable length and time scales, however, remain limited. In Monte Carlo simulations, the acceptance probability of displacements of polymers decreases with polymer size.^[25] Techniques to resolve these problems, such

1. Introduction

Developments in polymer science related to sustainable polymer materials result in a rapidly expanding number of possibilities for materials development, both in terms of new molecules like bio-based polymers^[1,2] and in terms of mixing different types of polymers in the circularity of polymers from post-consumer waste-streams.^[3,4] This development of new polymeric materials aims at tuning the molecular features to application demands. Different polymers, solvents, and fillers can be combined to

S. H. M. van Leuken, R. A. T. M. van Benthem, R. Tuinier, M. Vis
Laboratory of Physical Chemistry
Department of Chemical Engineering and Chemistry
Eindhoven University of Technology
P.O. Box 513, 5600 MB Eindhoven, The Netherlands
E-mail: r.tuinier@tue.nl; m.vis@tue.nl

S. H. M. van Leuken, R. Tuinier, M. Vis
Institute for Complex Molecular Systems
Eindhoven University of Technology
P.O. Box 513, 5600 MB Eindhoven, The Netherlands

 The ORCID identification number(s) for the author(s) of this article can be found under <https://doi.org/10.1002/mats.202300001>

© 2023 The Authors. Macromolecular Theory and Simulations published by Wiley-VCH GmbH. This is an open access article under the terms of the Creative Commons Attribution-NonCommercial License, which permits use, distribution and reproduction in any medium, provided the original work is properly cited and is not used for commercial purposes.

DOI: 10.1002/mats.202300001

as configuration-bias methods and the Pruned-enriched Rosenbluth method,^[26] only partially solve this problem and become unreliable for still relatively small molecules.^[25]

Simulations with larger polymers are possible using extended configurational bias methods such as the recoil-growth method^[27] and the Extended Continuum configurational bias method.^[28,29] For example, kink-jump and crankshaft,^[30,31] concerted rotation and bridging moves,^[32] or fractional moves^[33] also help to make simulations more efficient under specific conditions. The sampling efficiency can improve with, for example, pseudo-ensembles, parallel tempering, and histogram reweighting methods.^[21,25] Although these methods make simulations more efficient in certain situations, they are still inefficient for other cases, such as long chains.^[25] A higher number of molecular variations requires a higher number of polymers for proper sampling, resulting in even longer required computation times. Good initial guesses can reduce the required computation time. Direct, predictive theoretical expressions for the concentrations in phase-separated polymeric systems could deliver these initial guesses.

Numerical techniques are another way to estimate polymer phase stability. One of the most well-known theories to describe the phase stability of polymer mixtures is Flory–Huggins theory,^[8,34] which is generally solved numerically. This theory connects phase equilibria using a limited number of material-dependent variables for polymeric materials. In its mean-field description of polymers, Flory–Huggins theory assumes polymer segments distribute homogeneously. Also, it neglects the microstructure of polymers and only includes nearest-neighbor interactions. Despite the limitations of Flory–Huggins theory, trends in coexisting concentrations are well reflected by the theory.^[8] Other lattice theories and extensions of Flory–Huggins theory exist, reducing limitations and making the theory applicable in more situations. These extensions involve theories for the dependency of the interaction energy on environmental conditions and molecular features and adjustments of the used lattice statistics and spatial variations. Some examples are self-consistent field theory,^[35,36] cell theories,^[37] hole theories^[38,39] and local composition models.^[40,41] Although these techniques provide a fairly accessible way to predict the phase coexistence equilibria for many polymeric mixtures, making predictions becomes increasingly difficult with increasing complexity.

Compared with experiments, simulations, and numerical computations, direct analytical expressions can be quicker to use and more accessible for comparison with experiments. Additionally, such equations directly show how molecular features affect the miscibility of different components. These advantages help to interpret experimental data and guide polymer and material processing choices for circularity related applications. Moreover, researchers can fit analytical expressions with experiments, simulations, or numerical computations to find parameters and subsequently use these parameters to make predictions. For simulations and numerical computations, the direct analytical expressions can be used to determine the used initial guess.

This paper specifically focuses on Flory–Huggins theory to predict phase equilibria of polymeric systems. Flory–Huggins theory can be used to numerically determine binodals, which describe the equilibrium phase-separated concentrations. There is, however, not yet a direct, analytical expression for the bin-

odal that holds for the full range of concentrations. Several approximate analytical solutions, each applicable under specific conditions, to Flory–Huggins theory have been presented in the literature in the last few decades. For polymers with equal lengths, a Ginzburg–Landau expansion can be used to derive an approximate solution.^[42] The equilibrium absorption of infinitely long polymers in a bath of solvent without polymers can be estimated.^[43] Sanchez approximated the equilibrium concentrations for polymer mixtures close to the critical point.^[44] Scheinhardt-Engels, Leermakers, and Fleer^[45] derived equations near the critical point by requiring stationary diffusion between the different phases. Finally, Tsenoglou and Papaspyrides^[46] derived an analytical equation for mixtures where the two components are only slightly compatible, far from the critical point. Appendix A provides an overview of the expressions for the approximations from the literature.

Previous analytical expressions focused on specific conditions and limits. In contrast, in this paper, multiple analytical equations are presented that together describe the full range of possible interactions and polymer chain lengths. By providing analytical expressions for each step, from available coexisting concentrations to predictions for other coexisting concentrations, we give a more complete view than previously given in the literature. **Figure 1** gives a schematic overview of these different approximations *I–V*. In the different sections, expressions for specific limits are derived. These are used to relate a measured concentration directly to predicted concentrations in coexisting phases, relate a measured concentration to interaction parameters, and relate interaction parameters to predicted concentrations. Lower-order approximations can be used for more accessible analytical equations, useful for more intuitive insight into the system, or a higher-order approximation can be used to get more accurate predictions. In the following sections, we start with the theoretical background of Flory–Huggins theory, followed by the derivation of the approximate expressions. We first present expressions for a system consisting of two components, to make it easier to follow the derivations and to be able to compare directly with numerical results and approximations from literature. Next, the expressions are presented for multi-component systems for which numerical computations are challenging.

2. Theory

Flory–Huggins theory^[8,34] relates microscopic properties of polymers to the equilibrium concentrations in phase-separated polymer–polymer mixtures, polymer–solvent mixtures, and other polymer–small molecule mixtures. The Flory–Huggins Helmholtz energy *F* of mixing for two components reads

$$\frac{F}{Nk_B T} = \frac{\phi_1}{M_1} \ln \phi_1 + \frac{\phi_2}{M_2} \ln \phi_2 + \chi_{12} \phi_1 \phi_2 \quad (1)$$

with $N = M_1 N_1 + M_2 N_2$ the total number of lattice sites/monomers, k_B the Boltzmann constant, T the temperature, M_1 and M_2 the degree of polymerization of component 1 and 2, and χ_{12} the interaction parameter between components 1 and 2. The quantities $\phi_1 = \frac{M_1 N_1}{N}$ and $\phi_2 = \frac{M_2 N_2}{N}$ are the volume fractions of components of respectively type 1 and 2. Flory^[8] and Huggins^[34] derived this expression using a lattice approach

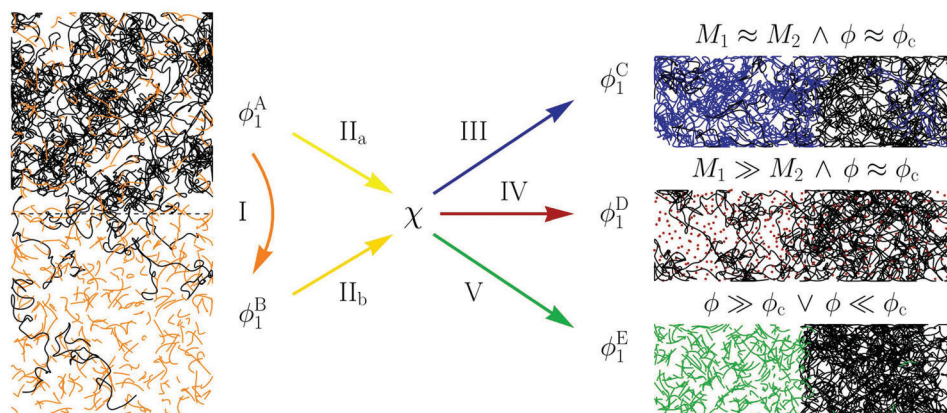


Figure 1. Schematic overview of the approximations. In approximation I, the concentration of component (1) in phase A (ϕ_1^A) can be used to determine the concentration in phase B (ϕ_1^B), which are in thermal, mechanical, and chemical equilibrium. Approximations II relate these concentrations in a closed expression to the interaction energies of the involved molecules (χ). The dependency of binodal concentrations on these interaction energies is given by approximations III–V. Approximations III and IV are valid when the components are miscible up to higher concentrations and approximation V holds when the components are only slightly miscible. Additionally, approximation III is valid when the involved polymers are similar in length, while approximation II applies when the chain lengths are significantly different.

which enabled them to express the entropy of mixing as well as the enthalpy of mixing of the components. The chemical potential μ of component 1 and 2 in a two component system are, from the derivative of the free energy Equation (1)

$$\frac{\mu_1^\alpha}{k_B T} = \ln \phi_1^\alpha + \left(1 - \frac{M_1}{M_2}\right) \phi_2^\alpha + M_1 \chi_{12} \phi_2^{\alpha 2} \quad (2)$$

$$\frac{\mu_2^\alpha}{k_B T} = \ln \phi_2^\alpha + \left(1 - \frac{M_2}{M_1}\right) \phi_1^\alpha + M_2 \chi_{12} \phi_1^{\alpha 2}$$

in all phases α . Two or more phases coexist if they are in thermal and mechanical equilibrium and if the chemical potentials of the different phases are equal, so for two components and two phases A and B

$$\mu_1^A = \mu_1^B \quad (3a)$$

$$\mu_2^A = \mu_2^B \quad (3b)$$

The Flory–Huggins lattice approach invokes incompressibility, so for two components volume conservation requires

$$\phi_1^A + \phi_2^A = 1 \quad (4a)$$

$$\phi_1^B + \phi_2^B = 1 \quad (4b)$$

Due to the assumed incompressibility, the osmotic pressure is directly related to the chemical potentials in Flory–Huggins theory. As a result, osmotic pressures are equal if the chemical potentials are equal.

The equations here are presented for unbranched homopolymers. When mean-field homogeneous mixing of groups can be assumed for copolymers, it is possible to average over all nearest-neighbor interactions, effectively averaging the contributions of

different groups. For example, for two copolymers a and b with n_a and n_b different groups

$$\chi_{ab}^* = \sum_i^{n_a} \sum_j^{n_b} \psi_i \psi_j \chi_{ij}^{ab} - \frac{1}{2} \sum_i^{n_a} \sum_i^{n_a} \psi_i \psi_j \chi_{ij}^{aa} - \frac{1}{2} \sum_i^{n_b} \sum_i^{n_b} \psi_i \psi_j \chi_{ij}^{bb} \quad (5)$$

In this equation, ψ_i and ψ_j are the volume fractions of groups i and j in the polymers. This effective interaction energy is the difference in interaction energy between the homogeneously mixed copolymers and phase separated copolymers, with in both states the different groups homogeneously mixed. The factors $\frac{1}{2}$ correct for double counting of interactions. Adaptations to this theory when homogeneous mixing cannot be assumed, for example for block-copolymers with large blocks, are out of the scope of this paper.

As a general analytical solution for the Flory–Huggins binodal does not exist, the system of Equations (2)–(4), is usually solved numerically. To test the analytical approximations for specific limits derived in this paper, we performed numerical computations using Wolfram Mathematica.^[47] To do these calculations, we solved Equations (2)–(4) using the function FindRoot.^[48] This function searches for a simultaneous numerical root of the given functions. The parameters were varied in small steps, starting at a state where each phase-consisted mostly of one component. For binary systems, this procedure suffices to find the numerical binodals. The reference dependencies plotted as grey lines in the figures in the next sections result from combining these numerical solutions. They are used to compare the predictions from analytical expressions and numerical computations. For systems with a higher number of components, these numerical computations would become more challenging and require appropriate initial guesses.

A point of a fluid–fluid binodal that can be found analytically is the critical point. This point marks the transition from the region where a mixture is stable at all concentrations to a region where phase-separation is possible. The critical point for a two

component mixture can be found by equating the second and third derivatives of F to ϕ to 0

$$\frac{\partial^2 F}{\partial \phi_1^2} = \frac{\partial^3 F}{\partial \phi_1^3} = 0 \quad (6)$$

In Section 3.1 we first focus on systems consisting of two components. As a result, there are either two phases or one mixed phase. For a binary mixture of components 1 and 2, the expression for the critical volume fraction of component 1 is

$$\phi_{c,1} = \frac{\sqrt{M_2}}{\sqrt{M_1} + \sqrt{M_2}} \quad (7)$$

which is used in some of the expressions derived in the next sections. In systems with many components, it is often possible to make additional approximations on the concentrations in the different phases. Section 3.2 gives three examples of such systems. Appendix A summarizes previously derived analytical approximations from literature^[42–46] in the same notation as our approximations.

3. Results and Discussion

3.1. Approximations for Two-Component Mixtures

In this section, approximations to Flory–Huggins theory are derived and tested. Although the dependency of the binodal concentrations can be determined readily for two components by numerically solving Equations (2)–(4), the case of two components makes the derivations more intuitive and easier to compare with numerical computations and previous approximations.^[42–46] In Section 3.2, the approximations presented here will be generalized to multi-component systems. The steps presented here cover the complete process from the input of measured concentrations to the required effective parameters and from the effective parameters to predictions for the concentrations in other systems.

3.1.1. Predicting Coexisting Concentrations Using Measured Concentrations

This section shows the derivation of an equation enabling the estimation of how much of a polymer is present in one phase based on that component's concentration in the other phase. Knowledge about the interaction parameter between the involved components is not needed. This equation can, for instance, be used to relate polymer dissolution to solvent uptake. At the same time, the effective ratio of polymer lengths, needed for predictive calculations, can be estimated from ϕ_1^A and ϕ_1^B because there is only one ratio for each combination of concentrations.

There are three limiting situations for which the coexistence concentrations for binary systems are known. The first one is the limit of complete phase-separation, $\phi_1^A = 1$ and $\phi_1^B = 0$ or $\phi_1^A = 0$ and $\phi_1^B = 1$. Second, when $M_1 = M_2$, symmetry dictates that $\phi_1^A = \phi_2^B$ and $\phi_2^A = \phi_1^B = 1 - \phi_2^B = 1 - \phi_1^A$, so $\phi_1^A + \phi_1^B = 1$ and $\phi_2^A + \phi_2^B = 1$. Finally, we can use that the concentrations are

known at the critical point (Equation (7)). As a possible equation satisfying these limits, valid for all M_1 and M_2 , we surmise

$$\phi_1^{A f_1(M_1, M_2)} + \phi_1^{B f_2(M_1, M_2)} = 1 \quad (8)$$

The functions f_1 and f_2 are yet to be determined, with the requirement that the real values of f_1 and f_2 are larger than zero. Due to the symmetry of the problem, ϕ_2^A and ϕ_2^B depend on M_2 and M_1 in the same way as ϕ_1^B and ϕ_1^A depend on M_1 and M_2 . Together with the requirement that $\phi_1^A = 1 - \phi_2^A$ and $\phi_1^B = 1 - \phi_2^B$, this yields

$$(1 - \phi_1^B)^{f_1(M_2, M_1)} + (1 - \phi_1^A)^{f_2(M_2, M_1)} = 1 \quad (9)$$

As a result of the chosen expression, the limits for full phase-separation and $M_1 = M_2$ are already satisfied. We can solve the set of Equations (8) and (9) by using the third limit, the critical point, Equation (7). Using this requirement in the equations above gives two equations that can be used to find f_1 and f_2

$$\phi_{c,1}^{f_1(M_1, M_2)} + \phi_{c,1}^{f_2(M_1, M_2)} = 1 \quad (10a)$$

$$(1 - \phi_{c,1})^{f_1(M_2, M_1)} + (1 - \phi_{c,1})^{f_2(M_2, M_1)} = 1 \quad (10b)$$

This set of equations has $f_1(M_1, M_2) = f_2(M_1, M_2) = -\log_2(\phi_{c,1}) = \log_2(1 + \sqrt{\frac{M_1}{M_2}})$ as a solution. This also means $f_1(M_2, M_1) = f_2(M_2, M_1) = \log_2(1 + \sqrt{\frac{M_2}{M_1}})$. Now, solving for ϕ_1^A or ϕ_1^B gives the following closed expression for the relation of the coexisting concentrations

$$\phi_1^A = \left(1 - \phi_1^{B/\epsilon}\right)^\epsilon \quad \text{with } \epsilon = \log_2\left(1 + \sqrt{\frac{M_1}{M_2}}\right) \quad (11)$$

$$\phi_1^B = \left(1 - \phi_1^{A/\epsilon}\right)^\epsilon$$

Figure 2 shows the difference between the numerical solutions of Flory–Huggins theory (grey curves) and Equation (11) (orange curves). The relation between the concentrations in the different phases is exact for $M_1 = M_2$, and closely resembles the dependencies for other values of $\frac{M_2}{M_1}$. Equation (11) suggests the proportionality of the concentrations in the different phases is only a function of the ratio of the polymer chain lengths and not of χ or the absolute lengths. Numerical computations with varying values for χ , M_1 and M_2 indeed confirm the independence of ϕ_1^B/ϕ_1^A of χ and the absolute values of M_1 and M_2 .

Equation (11) makes it possible to calculate how much of a component dissolves in one of two phase-separated phases by measuring the concentration in the other phase without needing any knowledge about the interaction energy between two components. Also, the effective ratio of the polymer lengths can be estimated using this equation. In Section 3.1.2, Equation (11) is used to derive a relation between the interaction energies and one of the concentrations, giving all parameters required to make predictions.

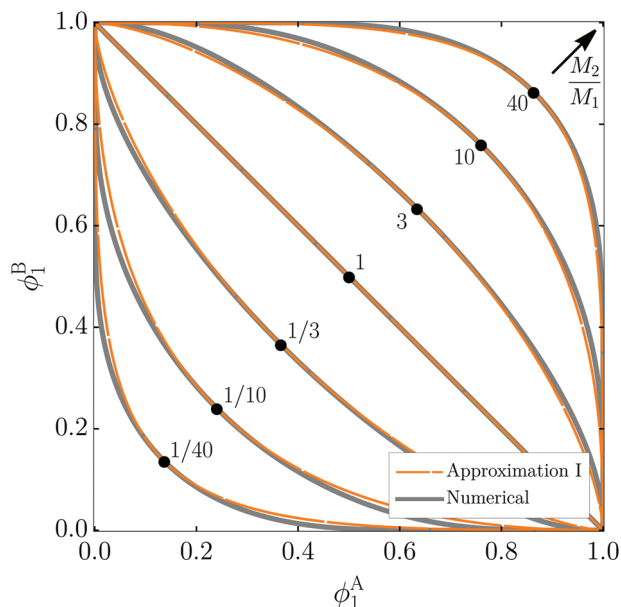


Figure 2. The relation between the binodal concentrations of component 1 in the two coexisting phases of a binary mixture. The grey curves show the numerical solutions at constant M_2/M_1 , the dashed orange curves follow the analytical expressions (approximation I, Equation (11)), and the dots show the critical points (Equation (7)).

3.1.2. Predicting Interaction Energies Using Measured Coexistence Concentrations

The equilibrium concentrations found in the coexisting phases of a particular two-component system can be used to calculate the phase equilibria of other mixtures with similar components. Interaction parameters can be used to perform these calculations, after these parameters are estimated. This section shows an analytical approximation of these interaction parameters χ as a function of the concentrations. With these equations, these wider applicable parameters can be determined directly from known concentrations.

Insertion of Equation (2) into Equations (3a) and (3b) gives

$$\chi = \frac{1}{M_2(\phi_1^A - \phi_1^B)} \left[\ln \frac{\phi_2^B}{\phi_2^A} + \left(1 - \frac{M_2}{M_1}\right)(\phi_1^B - \phi_1^A) \right] \quad (12a)$$

$$\chi = \frac{1}{M_1(\phi_2^B - \phi_2^A)} \left[\ln \frac{\phi_1^A}{\phi_1^B} + \left(1 - \frac{M_1}{M_2}\right)(\phi_2^A - \phi_2^B) \right] \quad (12b)$$

When all concentrations are known, these equations can be used directly. More conveniently, using the approximation presented in the previous section, it is only necessary to have one of these concentrations. ϕ_2^A and ϕ_2^B can be eliminated using $\phi_1^A + \phi_2^A = 1$ and $\phi_1^B + \phi_2^B = 1$. ϕ_1^A or ϕ_1^B can be eliminated using Equation (11). This results in equations relating χ directly to one of the coexisting concentrations

$$\chi = \frac{M_1 - M_2}{\phi_1^A + (1 - \phi_1^A)^{\epsilon}} + \frac{1}{M_2} \frac{\ln \left[\frac{1 - (1 - \phi_1^A)^{1/\epsilon}}{1 - \phi_1^A} \right]}{\phi_1^A - (1 - \phi_1^A)^{1/\epsilon}} \quad (13a)$$

$$\chi = \frac{M_1 - M_2}{[1 - \phi_1^B] + [1 - (1 - \phi_1^B)^{\epsilon}]^{\epsilon}} + \frac{1}{M_1} \frac{\ln \left[\frac{\phi_1^B}{(1 - \phi_1^B)^{\epsilon}} \right]}{[1 - \phi_1^B]^2 - [1 - (1 - \phi_1^B)^{1/\epsilon}]^2} \quad (13b)$$

In these equations, $\phi_1^A > \phi_{c,1}$ and $\phi_1^B < \phi_{c,1}$. For Equation (13a), the chemical potential of component 2 is used and ϕ_1^B is approximated using Equation (11), while in Equation (13b), the chemical potential of component 1 is used and ϕ_1^A is approximated using Equation (11). In both cases, the other balance of the chemical potentials is approximated indirectly using Equation (11). In one of the branch of the binodal, the first of these approximations has the largest effect, while in the other branch, the other approximation has the largest effect. Optimally, one of these equations is used for each of the branch of the binodal.

Figure 3 shows how these analytical expressions for χ as a function of a single binodal concentration compare with the numerical solution. For $M_1 = M_2$, both relations for χ are equal and exact, as the relation between ϕ_1^A and ϕ_1^B is exact. When M_1 and M_2 are not equal, and the best combination of approximations is used, the difference is smallest for high differences in length because the effect of the approximate relation between the concentrations derived in the previous section is smaller. The approximated binodal concentration has a smaller effect on χ for larger differences in length.

Interaction parameters χ of different polymers and solvents are used to compare and predict miscibilities. With Equation (13) interaction parameters can be calculated directly using a closed expression. Furthermore, χ can be estimated using only estimations of the lengths of the involved constituents and a single measured equilibrium phase concentration.

3.1.3. Predicting Coexisting Concentrations Using Interaction Energies

The microscopic properties of the polymers involved in a mixture can be used to predict phase coexistence concentrations. Conventionally, Equations (2)–(4) are used to numerically find the dependency of the binodal on M and χ . Especially for systems with many components, the process of solving Flory–Huggins equations requires appropriate initial guesses for the concentrations, and is further complicated by the larger number of variables. Furthermore, these relations accommodate the direct fitting of simulation and experimental data and quick calculations. Higher-order polynomial solutions are more accurate, and maintain the advantage that no initial guesses for the calculations are required. This section describes multiple relations of ϕ as a function of molecular features. The variance in approximations in

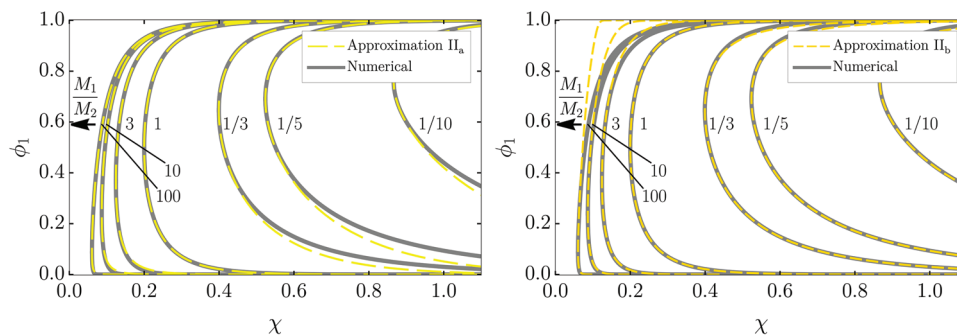


Figure 3. Binodals of binary mixtures for various chain length ratios M_1/M_2 with $M_2 = 10$. Numerical solutions are indicated by the solid grey curves. The yellow dashed curves are plotted using Equation (13a) (approximation II_a) in the left graph and using Equation (13b) (approximation II_b) in the right graph. For $\phi_1 > \phi_{c,1}$, Equation (13a) gives more accurate results, while for $\phi_1 < \phi_{c,1}$, Equation (13b) is more accurate.

distinct conditions renders the equations together applicable over a wide range of concentrations. Appendix B shows the derivations of these approximations. In this section, these approximations are presented for two components. In the next section, we will show that these approximations can be combined to determine concentrations for more than two components.

Phase Equilibria for Near-Critical Polymers with Equal and Similar Chain Lengths: When polymers with similar lengths are mixed, this can be described in Flory–Huggins theory with $M_1 \approx M_2$. These can be mixtures of smaller similar-sized polymers, such as monomers before a polymerization reaction or oligomer blends, or blends of larger polymers, where the difference in chain length is small relative to the absolute chain length of the mixed polymers. Up to second order, these symmetrical mixtures can be approximated as

$$\begin{aligned} \phi_1^A &= \frac{1}{2} + \frac{1}{2}\psi \\ \phi_1^B &= \frac{1}{2} - \frac{1}{2}\psi \end{aligned} \quad \text{with} \quad \psi = \sqrt{\frac{3}{2}M\chi - 3} \quad (14)$$

The derivation of this equation can be found in Appendix B.1. This solution is equal to the solution following from the Ginzburg–Landau expansion of the Flory–Huggins free energy.^[42] As expected, this equation suggests a critical point at $\psi = 0$, or $\chi = \frac{2}{M}$.

Figure 4 shows how Equation (14) and two higher-order approximations compare with numerical solutions to Flory–Huggins theory. Solutions for polynomials of all orders can be found using for example Horner’s method,^[49] the Secant method,^[50] or Brent’s method.^[51] With these methods, no prior knowledge about the system for initial guesses is necessary because variable intervals can be reduced until, in each interval, these methods are guaranteed to find the one valid solution.^[52] The agreement of the approximations is best for concentrations close to $\phi_{c,1}$. The range of χ -values where the approximation can be used is more extensive for shorter polymers because the concentrations are close to $\phi_{c,1}$ over a broader range of χ .

The same principle can be applied when M_1 and M_2 are not exactly equal, but similar. Using the precise values of M_1 and M_2 in the approximation, results in exactly $\phi_{c,1}$ in the limit $\psi \rightarrow 0$. The effect on the dependencies is, however, small for small differences in M . The next section discusses more accurate closed

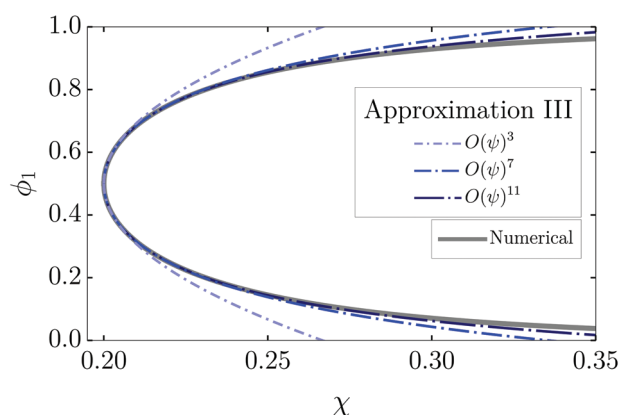


Figure 4. Binodal of the binary mixture with $M_1 = M_2 = 10$. Numerical solutions are indicated by the solid grey curves. The first blue dot-dashed curve is plotted using Equation (14). The darker, longer dashed curves are solutions using higher orders of Equation (B4).

expressions for larger differences in the polymer chain length. The limit $\psi \rightarrow 1$ is discussed in more detail in the final part of this section. This limit is relevant far from the critical point, where in each phase, the concentration of one of the components is much higher than the concentration of the other components.

Phase Equilibria for Near-Critical Polymers with Unequal Chain Lengths: This section focuses on systems with asymmetric chain lengths, where M_1 and M_2 are different. This situation is applicable in mixtures of a polymer and a solvent or mixtures of polymers that differ significantly in molar mass. An example of such a mixture is the combination of degraded and virgin polymer in a recycling process. Up to third order, these asymmetric mixtures can be approximated with

$$\phi_1^A = \phi_{c,1} + (1 - \phi_{c,1}) \left(-\frac{p_A}{2} + \sqrt{\left(\frac{p_A}{2}\right)^2 - \frac{q}{M_1}} \right) \quad (15a)$$

$$\phi_1^B = \phi_{c,1} - \phi_{c,1} \left(-\frac{p_B}{2} + \sqrt{\left(\frac{p_B}{2}\right)^2 - \frac{q}{M_2}} \right) \quad (15b)$$

Appendix B.2 shows the derivation of these equations. In these equations, $p_A = -\frac{3}{2}[2M_2(1 - \phi_{c,1})^2\chi - 1]$, $p_B = -\frac{3}{2}[2M_1\phi_{c,1}^2\chi - 1]$ and in both equations $q = 3[M_1\phi_{c,1} + M_2(1 - \phi_{c,1}) -$

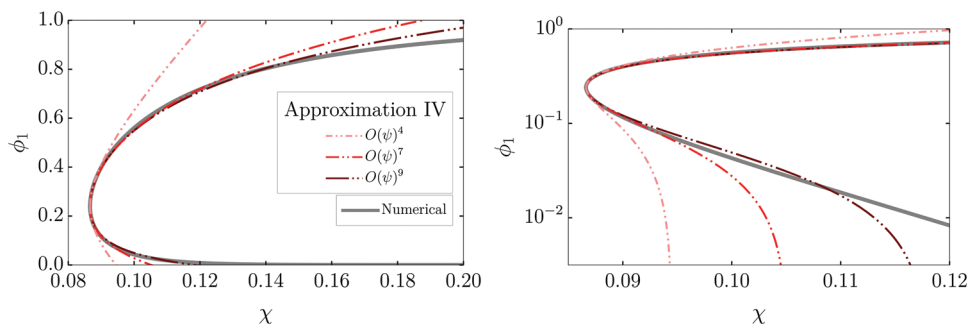


Figure 5. Linear and logarithmic plot of the binodal of the binary mixtures with $M_1 = 100$ and $M_2 = 10$. Numerical solutions are indicated by the solid grey curves. The first red double-dot-dashed curve is plotted using Equation (15). The darker, longer dashed curves are solutions that each use a higher-order of Equation (B9).

$2M_1M_2\phi_{c,1}(1-\phi_{c,1})\chi]$. Higher-order solutions can again be found using for example Horner's method,^[49] the Secant method,^[50] or Brent's method.^[51] **Figure 5** shows a linear and logarithmic plot of Equation (15) and two higher-order approximations compared to the numerical solutions. In the logarithmic plot it can be seen that increasing the order of the approximation does not always reduce the difference between the approximation and the numerical solution for a range of values of χ .

In the limit $M_1 \rightarrow \infty$ and $M_2 = 1$, Equation (15a) reduces to $\phi_1^A = 3(\chi - \frac{1}{2})$ and in the limit $M_1 \rightarrow 1$ and $M_2 = \infty$ Equation (15b), $\phi_1^B = 1 - 3(\chi - \frac{1}{2})$, which are the same limiting equations as found earlier.^[43] Far from the critical point, Equation (15) does not hold because the effect of the (smaller) change of one of the concentrations does not have a negligible effect far from the critical point. The limit $\psi \rightarrow 1$ is explained in more detail in the next section.

For both equal and unequal chain lengths, χ_c can already be used to directly determine whether polymer–polymer and polymer–solvent mixtures are miscible at all concentrations. The equations presented above for equal and unequal chain lengths make it possible to also directly estimate at which concentrations polymers are still miscible if χ is above χ_c . For phase-separating mixtures close to the critical point, the equations provide the equilibrium concentrations in each phase.

Phase Equilibria Far from the Critical Point: Finally, we show an approximate, closed expression for the binodal far from the critical point. This approximation can be used to find the equilibrium concentrations for mixtures with limited solubility. Examples of applications in this regime are determining whether fillers can be added to improve material properties, checking whether a polymeric material is susceptible to impurities or contaminants, and dilute polymeric systems. In such cases, the concentration dependency can be approximated with

$$\phi_1^A = \frac{1 - e^{-(\chi - \frac{1}{M_1})M_2 - 1}}{1 - e^{-(\chi - \frac{1}{M_1})M_2 - 1} e^{-(\chi - \frac{1}{M_2})M_1 - 1}} \quad (16a)$$

$$\phi_1^B = 1 - \frac{1 - e^{-(\chi - \frac{1}{M_2})M_1 - 1}}{1 - e^{-(\chi - \frac{1}{M_1})M_2 - 1} e^{-(\chi - \frac{1}{M_2})M_1 - 1}} \quad (16b)$$

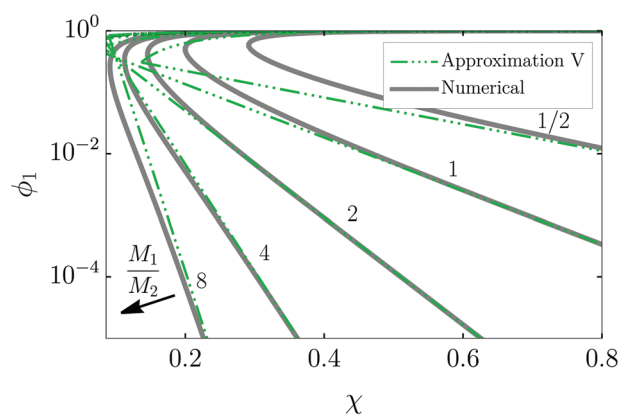


Figure 6. Binodal of the binary mixture with $M_2 = 10$. Numerical solutions are indicated by the solid grey curves. The green triple-dot-dashed curves are plotted using Equation (17) (approximation V).

This can be further simplified for large χ

$$\phi_1^A = 1 - e^{-(\chi - \frac{1}{M_1})M_2 - 1} \quad (17a)$$

$$\phi_1^B = e^{-(\chi - \frac{1}{M_2})M_1 - 1} \quad (17b)$$

Appendix B.3 shows the derivation of these equations. This equation can be confirmed with Equation (14) using the limit $\psi \rightarrow 1$ instead of $\psi \rightarrow 0$. A similar approach was used by Tsenoglou and Papaspyrides.^[46] The triple-dot-dashed curve in **Figure 6** shows how Equation (17) compare to the numerical solutions. For sufficiently large χ , the equilibrium concentrations also decrease exponentially with the length of the polymers. As expected, the binodal start deviating for smaller χ due to the approximations.

When $\chi = \frac{1}{M_1}$, the concentrations approach a constant, non-zero value for large M_2 that is independent of the chosen $\chi = \frac{1}{M_1}$. This can be understood by looking at the Flory–Huggins free energy (Equation (1)). When M_2 is large, the difference in entropy of the second constituent can be neglected. The equilibrium concentration of constituent 1 in phase A will be approximately 1. The total free energy is minimal when $\frac{dF}{dN_1} = 0$. At $\chi = \frac{1}{M_1}$, this condition reduces to $\ln(\phi_1^B) = -\phi_1^{B^2} + 3\phi_1^B - 2$, so $\phi_1^B = 0.3162$. Under these conditions, the entropy and enthalpy balance each

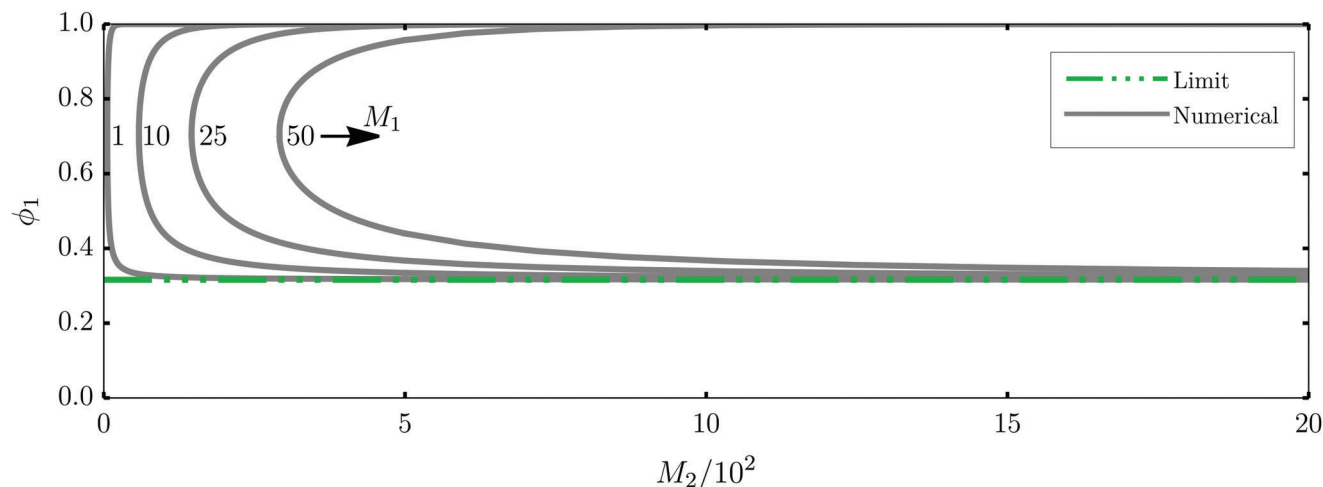


Figure 7. Numerical binodals of binary mixtures with $\chi = \frac{1}{M_1}$ (grey curves). For $\chi = \frac{1}{M_1}$, the concentration in one of the phases is expected to become independent of M_2 for large enough M_2 . This figure shows some examples of this effect. The green triple-dot-dashed curve is the theoretically expected limiting value of 0.3162.

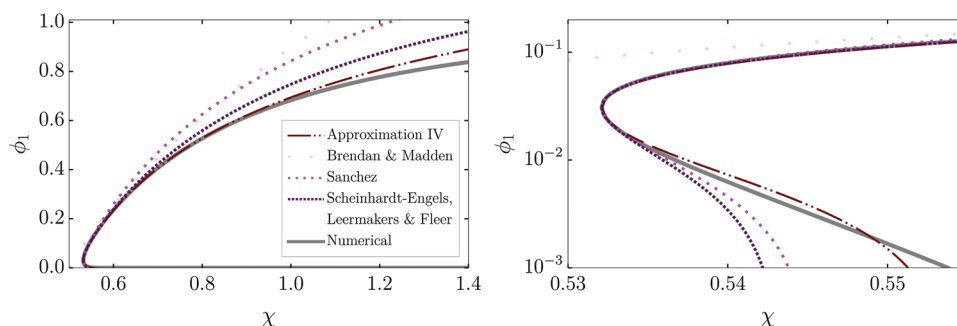


Figure 8. Linear and logarithmic plot of the binodal of the binary mixtures with $M_1 = 1000$ and $M_2 = 1$. Numerical solutions are indicated by the solid grey curves. The brown red double-dot-dashed curve is plotted using the same equation as the third curve in Figure 5. The purple dotted curves correspond to the approximations from literature, which can be found in Appendix A. Starting with the lightest color and largest distance between dots, the dots indicate the second approximation by Brennan and Madden (Equation (A2b)),^[43] the approximation by Sanchez,^[44] (Equation (A3)) and the approximation by Scheinhardt-Engels, Leermakers and Fleer (Equation (A5)).^[45]

other in such a way that the equilibrium concentration in phase B becomes independent of $\chi = \frac{1}{M_1}$ and M_2 .

Figure 7 illustrates that the concentrations approach a constant value for numerical solution of Flory–Huggins theory for $\chi = \frac{1}{M_1}$. This means that, in theory, it is possible to create a mixture where the degree of polymerization does not affect the equilibrium concentrations in the mixture. Experimentally, achieving such a combination of materials could ease the creation of materials with consistent properties, by decreasing the influence of for example polydispersity.

3.1.4. Combined Approximations and Comparison with Earlier Approximations

In the previous sections, we proposed approximate expressions for the binodal as a function of the material properties. Here we compare these results with previous findings by other groups.^[42–45] **Figure 8** compares the approximations for unequal

chain length in this paper, the earlier approximations, and the numerical solutions to Flory–Huggins theory. In this section, curves based on the derived equations in the previous sections are plotted with the same colors and dashing as in the earlier figures. For the higher-order approximations, it can be seen that our approach results in a smaller difference with the numerical solutions than the earlier approximations.

In **Figure 8**, the approximations explained in the other parts of this paper can be compared with the approximations from literature and the numerical solutions. Independent of M_1 and M_2 and the resulting location of the critical point, $\frac{d\phi_1^A}{d\phi_1^B} = -1$ at the critical point. This suggests an equidistant deviation of the two coexisting concentrations from the critical point by both branches of the binodal. Sanchez used an equidistant deviation in his derivation of an analytical expression of the Flory–Huggins concentrations as a function of the material properties.^[44] This approximation is expected to be more accurate close to the critical point than our approximation for symmetrical systems. The approaches described in this paper sacrifice some accuracy close to the

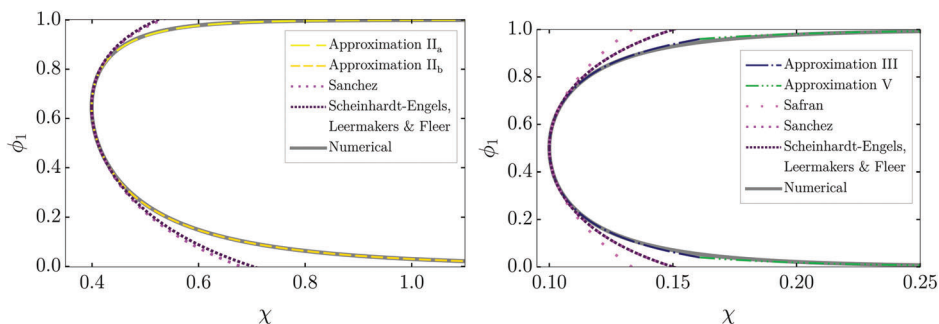


Figure 9. Binodals of the binary mixtures with $M_1 = 10$ and $M_2 = 3$ (left) and $M_1 = 20$ and $M_2 = 20$ (right). Numerical solutions are indicated by the solid grey curves. The pink dashed curves are a combination of Equation (13b) for $\phi_1 > \phi_{c,1}$ and Equation (13b) for $\phi_1 < \phi_{c,1}$. The blue dot-dashed curve and the green triple-dot-dashed curve are the same curves as in Figure 4 and Figure 6. The purple dotted curves correspond to the approximations from literature, which can be found in Appendix A. Starting with the lightest color and largest distance between dots, the symmetrical expansion by Safran (only in right graph, Equation (A1)),^[42] the approximation by Sanchez (Equation (A3)),^[44] and the approximation by Scheinhardt-Engels, Leermakers, and Fleer (left Equation (A5), right Equation (A4)).^[45]

critical point to win accuracy slightly further from the critical point. The approach also results in correct concentrations both in the limit close to the critical point ($\psi \rightarrow 0$, blue dot-dashed and green triple-dot-dashed curves) and infinity far from the critical point ($\psi \rightarrow 1$, green triple-dot-dashed curve).

The full range of concentrations can be approximated by combining (higher-order) approximations. **Figure 9** shows an example where Equations (13a) and (13b) are combined and where Equations (14) and (17) are combined. Combining the approximations mentioned in this paper, ϕ_1^A , ϕ_2^A , and χ can each be expressed in each other in closed expressions, both close to and far from the critical point.

3.2. Approximations for Multi-Component Mixtures

The previous sections show approximations of Flory–Huggins theory for two component mixtures and how they compare to numerical computations and earlier approximations. For such two-component systems, the number of concentrations that must satisfy the equations simultaneously is limited, making numerical determination straightforward. Computations becomes more demanding for multi-component systems due to the bigger system of equations and high number of concentrations that must be determined simultaneously. Computations become even more demanding when the different polymers vary in size and number of chemical groups. These properties affect the solubility and should be accounted in the calculations, increasing the number of components and equations even further.

With more components, Equations (2)–(4) and Equation (7) can be written as:

$$\frac{\mu_k^\alpha}{k_\beta T} = \ln(\phi_k^\alpha) + \sum_{i \neq k} \left[\left(1 - \frac{M_k}{M_i} \right) \phi_i^\alpha + M_k \chi_{ki} (1 - \phi_k^\alpha) \phi_i^\alpha - \frac{1}{2} M_k \sum_{j \neq k} \chi_{ij} \phi_i^\alpha \phi_j^\alpha \right] \quad (18a)$$

$$\mu_i^\alpha = \mu_i^\beta \quad (18b)$$

$$\sum_i \phi_i^\alpha = 1 \quad (18c)$$

$$\phi_{c,k} = \frac{\prod_{i \neq k} \sqrt{M_i}}{\sum_j \prod_{i \neq j} \sqrt{M_i}} \quad (18d)$$

In these equations, i, j , and k are indices of different components, and α and β are the indices of the different phases. The chemical potentials are now equal for all phases and all components. These are the equations needed to derive the approximate relations for multi-component mixtures.

Here, we demonstrate the advantage of the earlier discussed approximations using three examples of multi-components systems that are challenging to solve numerically without approximations. Many polymers have a large diversity of their chemical structure and chain lengths,^[53] drastically increasing the number of components. Despite its reported large affect,^[54] this variety is often not included in theoretical studies. The demonstrated procedure in the presented relatively simple conceptual examples can be applied in the same manner for more components, providing options for theoretical many-component studies.

3.2.1. Recycling Polymer Mixtures

As a first example, we focus on multi-component polymer mixtures in recycling processes. A way to maintain optimal properties for recycled materials is by separating different types of polymers during the recycling process. Using the difference in solubility of polymers is one of the techniques used for this separation.^[55,56] Although chemical differences in chemical groups in these materials make separation possible, this is never entirely without contaminations from other types of plastic. Therefore, minimizing the number of contaminations is desirable because their chemical structures can result in less favorable material properties and complicate the material's recycling process.^[56] For this reason, theoretically predicting how processing conditions affect the concentrations of these contaminations helps to improve polymer recycling but is challenging due to the number and variation in the components.

In the discussed situation, the different types of polymers each have limited miscibility in each other, so each phase will

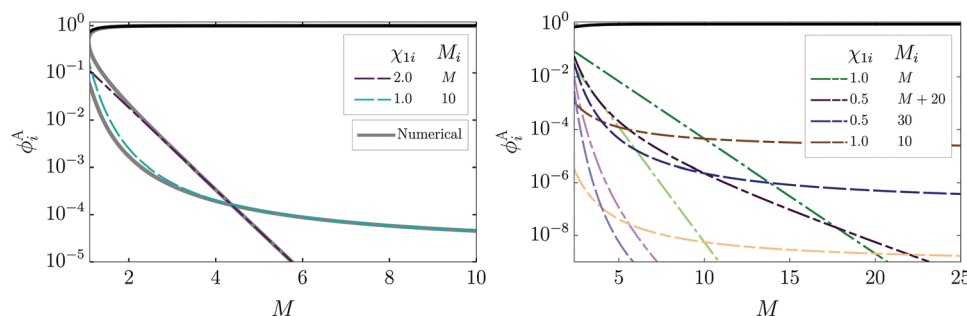


Figure 10. The concentrations of the different polymer types in one of the phases after separation in a recycling process. The left figure shows the analytical and numerical results for a hypothetical system with three components. The actual situation will be closer to the hypothetical system in the right figure, with nine components. The graphs show the effect of changing the length M of the common polymer 1 and two other polymers in phase A. All other polymer lengths are arbitrarily chosen. The lighter curves correspond to polymer with double the length of the polymers represented by the darker curves. The black curve is the concentration (ϕ^A) of the polymer at high concentration in phase A.

predominantly consist of one of the components. The concentration of the other components in that phase can be determined using a similar derivation as in Section 3.1.3. If we look at components 1 and 2 and phases A and B, where A is the phase with mostly 1 and B is the phase with mostly 2, we can neglect the concentrations of the other components 3, 4, 5, In this case, Equation (18) can again be simplified to Equation (B11) and from Equation (B11) to Equations (16) and (17), but with χ_{12} instead of χ . The same reasoning could be applied to the other phases and components, so in general

$$\phi_i^\beta = e^{-\left(\chi_{ij} - \frac{1}{M_j}\right)M_i - 1} \quad (19)$$

with j the majority component in phase β . The majority concentrations can be calculated after all the minority concentrations are determined using

$$\phi_j^\beta = 1 - \sum_{i \neq j} \phi_i^\beta \quad (20)$$

Figure 10 gives a hypothetical example of the recycled polymer mixture as a function of the size of these polymers. If the mixture consists of only of three components, numerical computations is still possible and can be compared with the approximations, resulting in Section 3.2.1. For all components, the approximations and numerical computations agree well further from the critical point. Closer to the critical point, the results deviate because limited miscibility is assumed. Section 3.2.1 shows a more realistic situation with nine components. In reality, there will be many more variations in lengths and number of functional groups in these polymers, resulting in an even greater number of components in the calculation. Using the approximations, the number of components has an insignificant effect on the difficulty of the calculations, while numerically solving the system of equations becomes very challenging.

3.2.2. Solvent Fractionation of Polydisperse Polymers

Solvent fractionation is selectively dissolving polymers with distinct properties such as size, composition, or structure. The technique is used in many forms in material preparation and

characterization.^[54,57] As an example of a polymer mixture in contact with a solvent mixture, we will look at the solvent fractionation of a polydisperse polymer in a solvent consisting of two components. We assume here that the total amount of solvent used is high in comparison to the total amount of polymer.

In the considered situation, the solvent molecules mix at all concentrations. As a result, the concentrations can be found directly from a mass balance. The effective interaction energy of the new, mixed, effective majority concentration of the mixed components m in phase β with the polymers i can be calculated using these concentrations

$$\chi_{i\beta}^* = \sum_m \theta_m^\beta \chi_{im} - \frac{1}{2} \sum_{m_1} \sum_{m_2} \theta_{m_1} \theta_{m_2} \chi_{m_1 m_2} \quad (21)$$

The interaction parameter $\chi_{i\beta}^*$ is the mean-field averaged interaction between polymer segment i and the solvent mixture with relative amounts θ_m . The relative numbers of interactions of i with different mixed components m scale with the relative amount of m . At the same time, a higher concentration of i results in a lower number of interactions between different mixed components m_1 and m_2 . The factor $\frac{1}{2}$ corrects for double counting of these interactions. This equation is a specific example of the effective interaction between mixtures

$$\chi_{ab}^{\alpha\beta} = \sum_i \sum_j \theta_i \theta_j \chi_{ij}^{\alpha\beta} - \frac{1}{2} \sum_i \sum_i \theta_i \theta_j \chi_{ij}^{\alpha\alpha} - \frac{1}{2} \sum_i \sum_i \theta_i \theta_j \chi_{ij}^{\beta\beta} \quad (22)$$

resulting from a mean-field comparison of the average number of interactions when the two blends are mixed with where the two components are in different phases. This equation is similar to Equation (5), for the effective averaging of functional groups.

The equation for the calculation of the equilibrium concentrations of the polymers is now equal to Equation (19), but with this effective interaction energy:

$$\phi_i^\beta = e^{-\left(\chi_{i\beta}^* - \frac{1}{M_j}\right)M_i - 1} \quad (23)$$

Figure 11 gives a hypothetical example of the equilibrium concentrations of a polydisperse polymer in the solvent mixture for

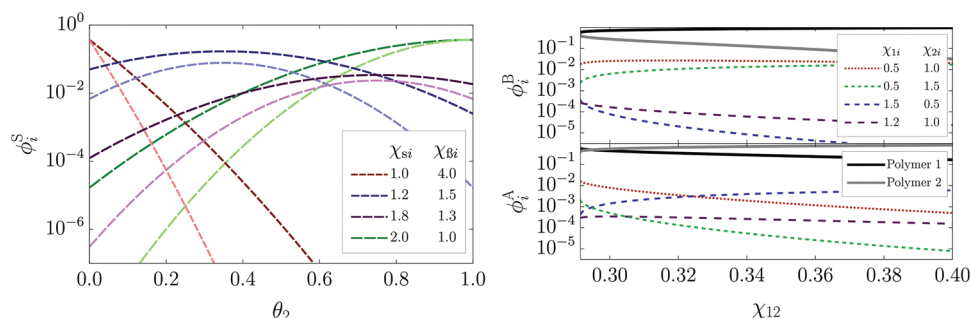


Figure 11. The left figure shows the maximal concentration of polymer that dissolves in a mixture of two solvents s and β as a function of the concentration of one of these two solvents. The right figure shows the concentration of additives and fillers as a function of the concentration of the interaction between two locally phase separated polymers in both phases. The interaction between the polymers 1 and 2 is varied, while the interactions between the polymers and the additives and fillers are kept constant.

eight different polymers. This graph shows that the maximal dissolving amount of polymer is larger for the shorter polymers in a polydisperse sample than for larger polymers. The concentration of a polymer can be maximal when θ_2 , the concentration of the second solvent, is minimal, maximal, or anywhere between these limits. Repeating this process in multiple solvents makes it possible to select polymers with certain lengths and functional groups. The same method can be used for polydisperse samples with a complete molar mass distribution.

3.2.3. Additives and Fillers in Polymer Blends

A polymer blend can be beneficial by combining each polymer's advantageous properties. Various additives and fillers are used to modify the properties of materials further. In some cases, mixtures of polymers will form a single, homogeneous phase, for which the concentrations of additives and fillers can be estimated similarly to Section 3.2.2. In other cases, local phase separation results in regions with a higher concentration of one of the mixed polymers. The equilibrium concentrations of the polymers, additives, and fillers in these phases influence each other.^[58,59] As a final example, we here consider a hypothetical system consisting of a mixture of two polymers that locally phase-separate, with small concentrations of additives and fillers, showing how the concentration of polymers in these phases affects the distribution of the additives and fillers over the phases.

In situations where there are components that have limited miscibility and components that have near-critical miscibility, first, the concentrations of components that have near-critical miscibility can be determined. For the calculation of these concentrations, the small concentrations of components with limited miscibility are neglected. If two of these near-critical components have similar lengths, their concentrations can be estimated using

$$\phi_1^\alpha = \frac{1}{2} + \frac{1}{2}\psi \quad (24a)$$

$$\phi_1^\beta = \frac{1}{2} - \frac{1}{2}\psi \quad (24b)$$

In the case of unequal chain lengths the concentrations can be approximated using

$$\phi_1^\alpha = \phi_{c,1} + (1 - \phi_{c,1}) \left(\sqrt{\left(\frac{p_\alpha}{2}\right)^2 - \frac{q}{M_1}} - \frac{p_\alpha}{2} \right) \quad (25a)$$

$$\phi_1^\beta = \phi_{c,1} \left(1 - \sqrt{\left(\frac{p_\beta}{2}\right)^2 - \frac{q}{M_2}} + \frac{p_\beta}{2} \right) \quad (25b)$$

or their higher order equivalents, following the logic in Section 3.1.3. This reasoning can be used for all the pairs of near-critical mixing phases in systems with even more phases. These equations can be used in the considered example to estimate the locally phase-separated polymers. After estimating these concentrations, again effective interaction energies can be estimated in each of these phases using Equation (22). The concentrations of the additives and fillers can then be estimated using

$$\phi_i^\beta = e^{-\left(\chi_{bi}^* - \frac{1}{M_b^*}\right)M_i - 1} \quad (26)$$

for each of the phases β . Besides the mean-field averaged interaction energy χ_{bi}^* , also the effective chain-length changes as a result of mixing, $M_b^* = \sum_j^{n_\beta} \frac{\phi_j^\beta}{M_j}$. This equation for M_b^* can be derived using the same steps as in Section 3.1.3, starting from Equation (18). The concentrations ϕ_j^β are the concentrations from Equations (24) and (25)

Section 3.2.2 shows how the distribution of the additives and fillers is affected by the relative concentrations of the polymers. These concentrations indirectly depend on the interaction of these two polymers. When the difference in polymer concentrations of the two phases is smaller, the difference in concentrations of the additives and fillers is also smaller. The same approach can be applied in numerically challenging systems with more coexisting phases, polymers, additives, and fillers.

4. Conclusions

Flory–Huggins theory can predict phase separation in mixtures of polymers and solvents. By equating the chemical potentials resulting from Flory–Huggins theory, the equilibrium compositions of the coexisting phases can be predicted numerically from the chain lengths and interactions of the involved molecules.

Especially for more complex mixtures, these numerical computations can be challenging compared to analytical approximations. Such approximations can be used to directly find interaction parameters by fitting experimental data using closed expressions, can be applied to calculate equilibrium concentrations quickly, and can provide initial values for numerical computations and simulations.

This paper gives an overview of different approximate, analytical solutions, each applicable in different situations. These situations include the miscibility of (bio-based) polymers and solvents, virgin and post-consumer polymers, and polymers and fillers, impurities or contaminants. The order of the used equations influences the accuracy but also the complexity of the calculations. The lower-order, closed expressions are simple and more convenient for quick calculation. Higher-order approximations are less readable, but more accurate and still free of a required initial guess. Combining the approximations makes it possible to make predictions over the full range of concentrations. The results show that close to the critical point, the logarithmic-terms in the equations for the chemical potentials can be approximated. When there is limited miscibility, all terms but the logarithmic terms can be approximated. Using the similarity or difference of the polymer chain lengths and the relation between the concentrations in different phases, the different concentrations and interaction energies can be connected with closed expressions.

The methods presented here can be applied to a mixture of any number of components. Here we demonstrated this for a multi-component polymer recycling mixture, polymer–solvent mixture after solvent fractionation and a mixture of polymers and additives and fillers. Depending on the considered system, different approximations can be combined, making it possible to predict phase equilibria for numerically challenging systems with multiple components, and with size polydispersity or chemical polydispersity. Together, the presented approximate relations between molecular features and equilibrium concentrations enhance the applicability of solvency theories by their simplicity and enhance their realistic relevance in practical circularity challenges by their extensibility.

Appendix A: Analytical Approximations to the Near-Critical Binodals from Flory–Huggins Theory from the Literature

This appendix presents a short overview of previous approximations of analytical expressions of binodals from Flory–Huggins theory. These solutions for the binodals are represented here using the same variables as used in this paper and are used for the literature results plotted in Figures 8 and 9.

A Ginzburg–Landau expansion^[42] can be used to derive an expression for the equilibrium concentrations as a function of the microscopic properties for a mixture of equal length polymers. In this approach, the entropic contribution to the free energy is expanded around the critical concentration, giving

$$\phi = \frac{1}{2} \pm \frac{1}{2} \sqrt{\frac{3}{2} M \chi - 3} \quad (\text{A1})$$

This equation is valid close to the critical point.

If polymers are in contact with a solvent, but the polymers do not dissolve in the solvent, the chemical potential of the solvent in the solvent-rich phase will be zero.^[43] This approximation is accurate for infinitely long polymers with positive interaction energies with small solvent molecules. If the logarithmic terms in the other chemical potential (see Equation (2)) are approximated using a Taylor expansion, an expression can be derived for the concentrations. The first- and second-order approximations by Brennan and Madden^[43] are given by

$$\phi = 3 \left(\chi - \frac{1}{2} \right) \quad (\text{A2a})$$

$$\phi = \frac{2}{3} \left(\sqrt{1 + 9 \left(\chi - \frac{1}{2} \right)} - 1 \right) \quad (\text{A2b})$$

Sanchez^[44] derived an equation for the concentrations as a function of the microscopic properties of materials. At the critical point, $\frac{d\phi_{1A}}{d\phi_{1B}} = -1$. This can be used to find

$$\phi = k_{\text{crit}} + \sqrt{3} (k - k_{\text{crit}}) \pm \frac{1}{2} b \sqrt{6} \quad (\text{A3a})$$

$$k = \frac{1}{2} + \frac{1}{4\chi} \left(\frac{1}{\sqrt{M_1}} - \frac{1}{\sqrt{M_2}} \right) \quad (\text{A3b})$$

$$k_{\text{crit}} = \frac{\sqrt{M_2}}{\sqrt{M_1} + \sqrt{M_2}} \quad (\text{A3c})$$

$$b^2 = 2k^2 - \frac{1}{\chi M_1} \quad (\text{A3d})$$

Scheinhardt-Engels, Leermakers, and Fleer^[45] derived equations using the flux of the components between the different states. In equilibrium, the net fluxes between the states should be zero, resulting in a set of equations that can be solved close to the critical point. They used the Flory–Huggins chemical potentials for the flux. For mixtures with equal chain length, they found

$$\phi = k \pm \frac{1}{2} b \sqrt{6} \quad (\text{A4a})$$

$$k = \frac{1}{2} + \frac{1}{4\chi} \left(\frac{1}{\sqrt{M_1}} - \frac{1}{\sqrt{M_2}} \right) \quad (\text{A4b})$$

$$b^2 = 2k^2 - \frac{1}{\chi M_1} \quad (\text{A4c})$$

For polymers with different chain lengths

$$\phi = \frac{1}{2} \left(3k - k_{\text{crit}} \pm \sqrt{6b^2 - 3(k - k_{\text{crit}})^2} \right) \quad (\text{A5a})$$

$$k = \frac{1}{2} + \frac{1}{4\chi} \left(\frac{1}{\sqrt{M_1}} + \frac{1}{\sqrt{M_2}} \right) \quad (\text{A5b})$$

$$b^2 = 2k^2 - \frac{1}{\chi M_1} \quad (\text{A5c})$$

Appendix B: Derivations of Coexisting Concentrations as a Function of Interactions Energies

B.1. Mixtures of Near-Critical Polymers with Equal and Similar Chain Lengths

Here an approximate relation relating coexistence concentrations to M and χ for polymers with similar chain lengths is presented. We introduce a new variable, ψ , that attains a value $\psi = 0$ at the critical point ($\chi \rightarrow \chi_c$) and $\psi = 1$ infinitely far from the critical point ($\chi \rightarrow \infty$). In the second of these limits, all ϕ 's go to either 1 or 0. For (approximately) symmetric systems

$$\phi_1^A = \phi_{c,1} + (1 - \phi_{c,1})\psi \quad (\text{B1a})$$

$$\phi_1^B = \phi_{c,1} - \phi_{c,1}\psi \quad (\text{B1b})$$

with $0 \leq \psi \leq 1$. Next, a connection is made with the molecular features χ and M . If the expressions are used in Equation (12a), it reduces to

$$\chi = \frac{\left(1 - \frac{M_2}{M_1}\right)\psi + \ln\left(\frac{[1-\phi_{c,1}]+\phi_{c,1}\psi}{[1-\phi_{c,1}]-[1-\phi_{c,1}]\psi}\right)}{M_1\left([\phi_{c,1} + (1 - \phi_{c,1})\psi]^2 - [\phi_{c,1} - \phi_{c,1}\psi]^2\right)} \quad (\text{B2})$$

For symmetrical systems ($M_1 = M_2$), which have their critical point at $\phi_{c,1} = \frac{1}{2}$

$$M\chi = \frac{1}{\psi} \ln\left(\frac{\frac{1}{2} + \frac{1}{2}\psi}{\frac{1}{2} - \frac{1}{2}\psi}\right) \quad (\text{B3})$$

Using Equation (12b) instead of Equation (12a) in the derivation gives the same result (Equation (B3)). To obtain an expression with ϕ as a function of the material properties close to the critical point, one can use a series expansion of the logarithmic term around $\psi \approx 0$, giving

$$\ln\left(\frac{\frac{1}{2} + \frac{1}{2}\psi}{\frac{1}{2} - \frac{1}{2}\psi}\right) \approx \sum_{i=0}^k \frac{2}{2i+1} \psi^{2i+1} \quad (\text{B4})$$

The higher k , the higher the precision of the resulting equation, and for $k = \infty$ Equation (B4) is exact. For example, up to 2nd order in ψ ($k = 1$), the resulting equation is

$$M\chi = 2 + \frac{2}{3}\psi^2 \quad (\text{B5a})$$

and solving for ψ and using Equation (B1) gives Equation (14).

B.2. Mixtures of Near-Critical Polymers with Unequal Chain Lengths

This section shows the derivation of an approximate relation relating coexistence concentrations to M and χ for polymers with unequal chain lengths. As a result of the asymmetrical binodal in these cases, one of the coexisting concentrations varies strongly with χ , while the other concentration varies weakly with χ . In the limit $M_1 \gg M_2$ and in the limit $M_2 \gg M_1$, the concentration at the critical point $\phi_{c,1} \approx 0$ for one of the constituents and $1 - \phi_{c,1} \approx 1$ for the other constituent. The concentration that is already close to its limiting concentration will not change much with χ . We use this to approximate the concentration dependency with

$$\phi_1^A = \phi_{c,1} + (1 - \phi_{c,1})\psi \quad (\text{B6a})$$

$$\phi_1^B = \phi_{c,1} \quad (\text{B6b})$$

for $\phi_{c,1} \approx 0$, or

$$\phi_1^A = \phi_{c,1} \quad (\text{B7a})$$

$$\phi_1^B = \phi_{c,1} - \phi_{c,1}\psi \quad (\text{B7b})$$

for $\phi_{c,1} \approx 1$.

The quantity ψ is chosen such that the concentrations are equal to the concentrations at the critical point for $\psi = 0$. Using Equations (B6) and (B7) in Equations (13a) and (13b) gives

$$\chi = \frac{(M_2 - M_1)(1 - \phi_{c,1})\psi + M_1 \ln\left(\frac{1}{1-\psi}\right)}{M_1 M_2 \left([\phi_{c,1} + (1 - \phi_{c,1})\psi]^2 - \phi_{c,1}^2\right)} \quad (\text{B8a})$$

$$\chi = \frac{(M_1 - M_2)\phi_{c,1}\psi + M_2 \ln\left(\frac{1}{1-\psi}\right)}{M_1 M_2 \left([1 - \phi_{c,1}]^2 - [(1 - \phi_{c,1}) + \phi_{c,1}\psi]^2\right)} \quad (\text{B8b})$$

with $\phi_1^A > \phi_{c,1}$ for Equation (B8a) and $\phi_1^B < \phi_{c,1}$ for Equation (B8b).

The logarithmic terms can again be replaced with a series expansion around $\psi = 0$

$$\ln\left(\frac{1}{1-\psi}\right) \approx \sum_{i=1}^k \frac{\psi^i}{i} \quad (\text{B9})$$

which is exact for $k = \infty$. Approximating Equations (B8a) and (B8b) to third order in ψ and solving for ψ results in Equation (15).

B.3. Derivation for Mixtures of Polymers with Limited Miscibility

Here we present the derivation for the equilibrium concentrations of slightly mixing polymers. The starting point of this derivation is Equations (2)–(4). Using the expressions for the chemical potentials in Equation (2) and in Equation (3) and rearranging gives

$$\ln \frac{\phi_1^B}{\phi_1^A} = \left[\left(1 - \frac{M_1}{M_2}\right) \phi_2^A + M_1 \chi \phi_2^{A^2} \right] - \left[\left(1 - \frac{M_1}{M_2}\right) \phi_2^B + M_1 \chi \phi_2^{B^2} \right] \quad (\text{B10a})$$

$$\ln \frac{\phi_2^A}{\phi_2^B} = \left[\left(1 - \frac{M_2}{M_1}\right) \phi_1^B + M_2 \chi \phi_1^{B^2} \right] - \left[\left(1 - \frac{M_2}{M_1}\right) \phi_1^A + M_2 \chi \phi_1^{A^2} \right] \quad (\text{B10b})$$

Far from the critical point ($\chi \gg \chi_c$), both phases consist mostly of one of the components. If we arbitrary choose that phase A is rich in component 1 and phase B rich in component 2, we can assume $\phi_1^A \gg \phi_2^A$ and $\phi_1^B \ll \phi_2^B$. This also means $\phi_1^A = 1 - \phi_2^A \approx 1$, $\phi_2^A \approx 0$, $\phi_1^B \approx 0$, and $\phi_2^B = 1 - \phi_1^B \approx 1$. The absolute value of both logarithmic terms of Equation (B10) go to plus or minus infinity if the ratio between the concentrations goes to zero or infinity ($\ln \frac{1}{0} = \infty$ and $\ln \frac{0}{1} = -\infty$). On the right-hand side of the equation, the difference between using $\phi_1^A = 1$, $\phi_2^A = 0$, $\phi_1^B = 0$, and $\phi_2^B = 1$ and the slightly different, not approximated coexistence concentrations is small, so equation B10 can be approximated as

$$\frac{\phi_1^B}{\phi_1^A} = e^{-\left(\chi - \frac{1}{M_2}\right)M_1 - 1} \quad (\text{B11a})$$

$$\frac{\phi_2^A}{\phi_2^B} = e^{-\left(\chi - \frac{1}{M_1}\right)M_2 - 1} \quad (\text{B11b})$$

This corresponds to neglecting all but the zeroth-order terms in a Taylor expansion of the right-hand side of Equation (B10) around $\phi_2^A \approx 0$ and $\phi_1^B \approx 0$. Equation (B11) can be solved algebraically for ϕ_1^A and ϕ_1^B , by using that $\phi_1^A = 1 - \phi_2^A$ and $\phi_2^B = 1 - \phi_1^B$, giving Equation (16).

Acknowledgements

This work was performed within the framework of the public-private knowledge institute of Chemelot InSciTe, which the authors gratefully acknowledge for their financial support. Furthermore, the authors would like to thank the members of the Chemelot InSciTe HiperBioPol-team and the members of the Laboratory of Physical Chemistry at Eindhoven University of Technology for the discussions, inspiration, and feedback.

Conflict of Interest

The authors declare no conflicts of interest.

Data Availability Statement

The data that support the findings of this study are available from the corresponding author upon reasonable request.

Keywords

analytical, approximations, binodal, Flory–Huggins, miscibility, solution theory, solvency

Received: January 11, 2023

Revised: February 21, 2023

Published online: March 20, 2023

- [1] M. L. Di Lorenzo, R. Androsch, *Thermal Properties of Bio-Based Polymers*, Springer, Cham **2019**.
- [2] R. P. Babu, K. O'Connor, R. Seeram, *Prog. Biomater.* **2013**, *2*, 8.
- [3] A. Dorigato, *Adv. Ind. Eng. Polym. Res.* **2021**, *4*, 53.
- [4] K. Hamad, M. Kaseem, F. Deri, *Polym. Degrad. Stab.* **2013**, *98*, 2801.
- [5] K. Pajula, M. Taskinen, V.-P. Lehto, J. Ketolainen, O. Korhonen, *Mol. Pharm.* **2010**, *7*, 795.
- [6] T. L. Hill, J. W. Rowen, *J. Polym. Sci.* **1952**, *9*, 93.
- [7] S. Vanhee, R. Koningsveld, H. Berghmans, K. Šolc, W. H. Stockmayer, *Macromolecules* **2000**, *33*, 3924.
- [8] P. J. Flory, *J. Chem. Phys.* **1941**, *10*, 51.
- [9] R. Mohan, H. Lorenz, A. S. Myerson, *Ind. Eng. Polym. Res.* **2002**, *41*, 4854.
- [10] A. F. Halasa, G. D. Wathen, W. L. Hsu, B. A. Matrana, J. M. Massie, *J. Appl. Polym. Sci.* **1991**, *43*, 183.
- [11] J. L. White, M. Wachowicz, *Annu. Rep. NMR Spectrosc.* **2008**, *64*, 189.
- [12] S. Sheokand, S. R. Modi, A. K. Bansal, *J. Pharm. Sci.* **2014**, *103*, 3364.
- [13] P. Munk, P. Hattam, A.-A. A. Abdel-Azim, Q. Du, in *Macromolecular Symposia*, Vol. 38, Wiley, New York **1990**, pp. 205–220.
- [14] P. B. Rim, J. P. Runt, *Macromolecules* **1984**, *17*, 1520.
- [15] M. Jiang, W. Chen, T. Yu, *Polymer* **1991**, *32*, 984.
- [16] S. N. Semerak, C. W. Frank, *Macromolecules* **1981**, *14*, 443.
- [17] S. Thomas, Y. Grohens, P. Jyotishkumar, *Characterization of Polymer Blends: Miscibility, Morphology and Interfaces*, Wiley, New York **2014**.
- [18] L. Robeson, *Polymers* **2014**, *6*, 1251.
- [19] R. Dohrn, J. M. S. Fonseca, S. Peper, *Annu. Rev. Chem. Biomol. Eng.* **2012**, *3*, 343.
- [20] F. A. Escobedo, J. J. De Pablo, *Phys. Rep.* **1999**, *318*, 85.
- [21] A. Z. Panagiotopoulos, *J. Phys. Condens. Matter* **2000**, *12*, R25.
- [22] M. Doi, S. F. Edwards, S. F. Edwards, *The Theory of Polymer Dynamics*, Oxford University Press, Oxford **1988**.
- [23] Y. I. Yang, Q. Shao, J. Zhang, L. Yang, Y. Q. Gao, *J. Chem. Phys.* **2019**, *151*, 070902.
- [24] K. Binder, *Monte Carlo and Molecular Dynamics Simulations in Polymer Science*, Oxford University Press, Oxford **1995**.
- [25] J. J. de Pablo, Q. Yan, F. A. Escobedo, *Annu. Rev. Phys. Chem.* **1999**, *50*, 377.
- [26] P. Grassberger, *Phys. Rev. E* **1997**, *56*, 3682.
- [27] S. Consta, N. B. Wilding, D. Frenkel, Z. Alexandrowicz, *J. Chem. Phys.* **1999**, *110*, 3220.
- [28] F. A. Escobedo, J. J. de Pablo, *J. Chem. Phys.* **1996**, *104*, 4788.
- [29] M. Vendruscolo, *J. Chem. Phys.* **1997**, *106*, 2970.
- [30] P. H. Verdier, W. H. Stockmayer, *J. Chem. Phys.* **1962**, *36*, 227.
- [31] M. Lax, C. Brender, *J. Chem. Phys.* **1977**, *67*, 1785.
- [32] V. G. Mavrantzas, T. D. Boone, E. Zervopoulou, D. N. Theodorou, *Macromolecules* **1999**, *32*, 5072.
- [33] A. Rahbari, R. Hens, I. K. Nikolaidis, A. Poursaidesfahani, M. Ramdin, I. G. Economou, O. A. Moulto, D. Dubbeldam, T. J. H. Vlucht, *Mol. Phys.* **2018**, *116*, 3331.
- [34] M. L. Huggins, *J. Chem. Phys.* **1941**, *9*, 440.
- [35] J. M. H. M. Scheutjens, G. J. Fleer, *J. Phys. Chem.* **1979**, *83*, 1619.
- [36] J. M. H. M. Scheutjens, G. J. Fleer, *J. Phys. Chem.* **1980**, *84*, 178.
- [37] I. Prigogine, V. Mathot, *J. Chem. Phys.* **1952**, *20*, 49.
- [38] A.-V. G. Ruzette, A. M. Mayes, *Macromolecules* **2001**, *34*, 1894.
- [39] R. Simha, T. Somcynsky, *Macromolecules* **1969**, *2*, 342.
- [40] G. Maurer, J. M. Prausnitz, *Fluid Ph. Equilibria* **1978**, *2*, 91.
- [41] J. Gmehling, J. Li, M. Schiller, *Ind. Eng. Chem. Res* **1993**, *32*, 178.
- [42] S. A. Safran, *Statistical Thermodynamics of Surfaces, Interfaces, and Membranes*, CRC Press, Boca Raton, FL **2018**.
- [43] J. K. Brennan, W. G. Madden, *Macromolecules* **2002**, *35*, 2827.
- [44] I. C. Sanchez, *Macromolecules* **1984**, *17*, 967.
- [45] S. M. Scheinhardt-Engels, F. A. M. Leermakers, G. J. Fleer, *Phys. Rev. E* **2004**, *69*, 021808.
- [46] C. J. Tsenoglou, C. D. Pappaspyrides, *Polymer* **2001**, *42*, 8069.
- [47] Wolfram Research, Inc., Wolfram|Alpha knowledgebase, Champaign, IL, **2018**.
- [48] Wolfram Research, FindRoot, <https://reference.wolfram.com> (accessed: February 2023).
- [49] W. G. Horner, *Philos. Trans. Royal Soc.* **1819**, *109*, 308.
- [50] W. H. Press, S. A. Teukolsky, W. T. Vetterling, B. P. Flannery, *Numerical Recipes in Fortran 90*, Cambridge University Press, Cambridge **1996**.
- [51] R. P. Brent, *Algorithms for Minimization without Derivatives*, Prentice-Hall, Englewood Cliffs, NJ **1973**.
- [52] R. P. Brent, *Comput. J.* **1971**, *14*, 422.
- [53] P. E. Slade, *Polymer Molecular Weights*, Vol. 4, CRC Press, Boca Raton, FL **1975**.
- [54] M. J. Cantow, *Polymer Fractionation*, Elsevier, New York **2013**.
- [55] B. Ruj, V. Pandey, P. Jash, V. Srivastava, *Int. J. Appl. Sci. Eng. Res* **2015**, *4*, 564.
- [56] D. Froelich, E. Maris, N. Haoues, L. Chemineau, H. Renard, F. Abraham, R. Lassartesses, *Miner. Eng.* **2007**, *20*, 902.
- [57] F. Francuskiewicz, *Polymer Fractionation*, Springer, Berlin, Heidelberg **2013**.
- [58] A. Karim, D.-W. Liu, J. F. Douglas, A. Nakatani, E. J. Amis, *Polymer* **2000**, *41*, 8455.
- [59] J. Dudowicz, K. F. Freed, J. F. Douglas, *Macromolecules* **1995**, *28*, 2276.